Spherical Horn Array for Wideband Propagation Measurements

Franek, Ondrej; Pedersen, Gert Frølund

Published in:
I E E E Transactions on Antennas and Propagation

DOI (link to publication from Publisher):
10.1109/TAP.2011.2152349

Publication date:
2011

Document Version
Accepted author manuscript, peer reviewed version

Spherical Horn Array for Wideband Propagation Measurements

Ondřej Franek, *Member, IEEE,* and Gert Frølund Pedersen

***Abstract*—A spherical array of horn antennas designed to obtain directional channel information and characteristics is introduced. A dual-polarized quad-ridged horn antenna with open flared boundaries and coaxial feeding for the frequency band 600 MHz–6 GHz is used as the element of the array. Matching properties and coupling between the elements are investigated via measurements and numerical simulations. Radiation patterns and sum beams of the array on selected frequencies throughout the band are also presented. Based on the obtained results it is concluded that the array is a good candidate for a wideband multipath propagation studies.**

***Index Terms*—Antenna arrays, antenna array mutual coupling, horn antennas**

I. Introduction

In order to measure the propagation channel characteristics without antenna influence and extensive postprocessing, a spherical array of antennas is needed. The elements of the array should theoretically have medium gain, both polarizations, and cover wide frequency range. Also, in order to directly retrieve the directional channel information and to obtain sufficiently isotropic coverage, we need moderately narrow radiation beam covering the whole sphere. One possibility is to use a directional antenna with the desired characteristics on a pedestal, scanning the space to obtain directional information [1], but this solution cannot accommodate the velocities typically involved in mobile experiments. Fast and simultaneous measurements are, however, feasible with spherical arrays. A spherical array composed of microstrip patch antennas was introduced in [2], but the bandwidth offered by this type of antennas is generally poor.

In our previous measurement campaign, we used a spherical array of monopoles [3] with the view of increasing the bandwidth. Although successful in some aspects, it did not allow a simple estimation of directional information because the elements of the array, monopoles, were not directional, instead having maximum radiation around the circumference. This made the determination of signal direction particularly difficult in terms of postprocessing. For the next measurement campaign we therefore decided to use horn antennas to compose the array.

Horn antennas are well known for being used as primary reflector feeds, in electromagnetic compatibility measurements and for standard gain calibration purposes [4]. Their main advantages are relatively wide bandwidth, high gain, and the possibility to accommodate both polarizations within one antenna. The bandwidth can be further enlarged by introducing ridges, which, together with symmetrical feeding, substantially extend the waveguide single-mode operation [5]. As our measurement campaigns were expected to require wideband measurements from 600 MHz to 6 GHz (i.e. LTE interfaces span from 700 MHz up to 2.7 GHz) as well as both polarizations, we decided to use the ridged design with dual polarization, i.e. quadruple-ridged horn antenna.

Double ridged horn antennas have been studied widely in the literature, for examples we refer to [6]–[9]. Publications on quad-ridged horns, on the other hand, are few. An early presentation of quad-ridged design, although very brief, can be found in [10]. A dual-polarized ridged horn with coaxial feeding and bandwidth from 2 to 26.5 GHz was introduced in [11]. Another original design was presented in [12], where the quad-ridged horn intended for anechoic chamber operation in 2–18 GHz band was stripped off the flare boundaries while maintaining very good radiation and matching parameters. Recently, two novel designs of quad-ridged horn antennas, with full flare boundaries though, were presented in [13] and [14], with respective bandwidths 8–18 GHz and 2–18 GHz and coaxial feeding. However, none of the papers addressed the possibility of using such antenna as an array element.

In this paper, we introduce a spherical array of quad-ridged dual-polarized horn antennas with frequency range 600 MHz-6 GHz. Focus is given on aspects relevant to using this array for obtaining channel characteristics and directional information. In particular, we present reflection coefficient (s_{11}), coupling (s_{21}) and radiation patterns. The data were obtained from anechoic chamber measurements and from simulation by the finite-difference time-domain (FDTD) method [15].

II. Description

A. The Antenna

The element of the proposed array is a diagonal horn antenna with four ridges added for simultaneous use of both vertical and horizontal polarizations (see Figs. 1 and 2). The initial design of the horn antenna has been prepared using simulations in our in-house FDTD code. Optimization has been performed by sweeping through many values for the feed position, the gap between the ridges, the thickness of the ridges, the chamfering angle near the feed, and the position of the shorting strip. The optimization had strong

Manuscript received August 18, 2010; revised December 2, 2010. This work was supported by the Danish Center for Scientific Computing.

O. Franek and G. F. Pedersen are with the Antennas, Propagation and Radio Networking section, Department of Electronic Systems, Aalborg University, DK-9220 Aalborg Øst, Denmark (e-mail: franek@ieee.org, gfp@es.aau.dk)

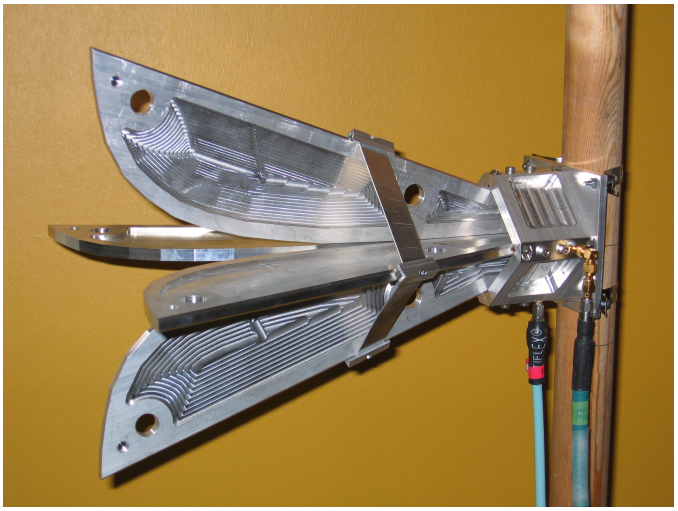

Fig. 1. The realization of the quad-ridged dual-polarized horn antenna.

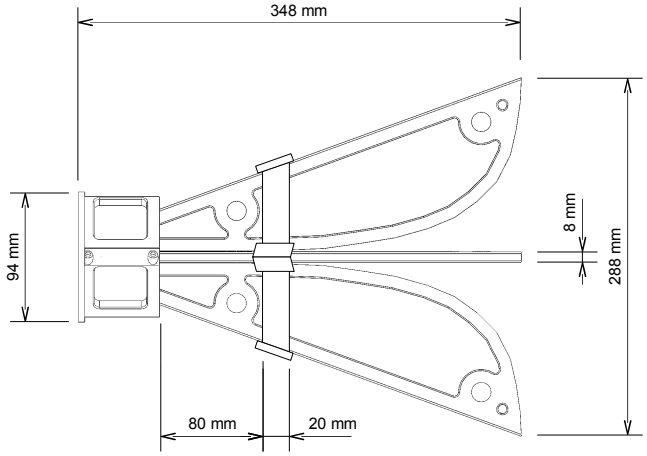

Fig. 2. Dimensions of the horn antenna.

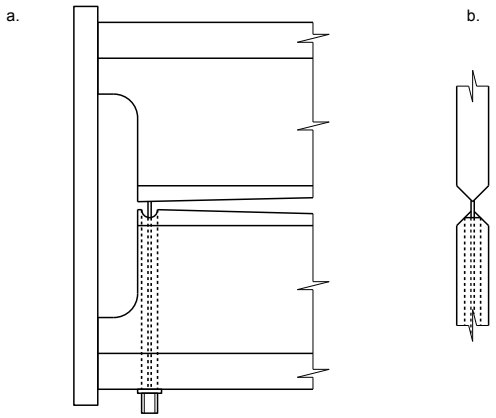

Fig. 3. Detail of the feed with two ridges present: a. side-view, b. cross-section. Arrangement of the perpendicular ridges is similar, only the feed is shifted 2 mm forward.

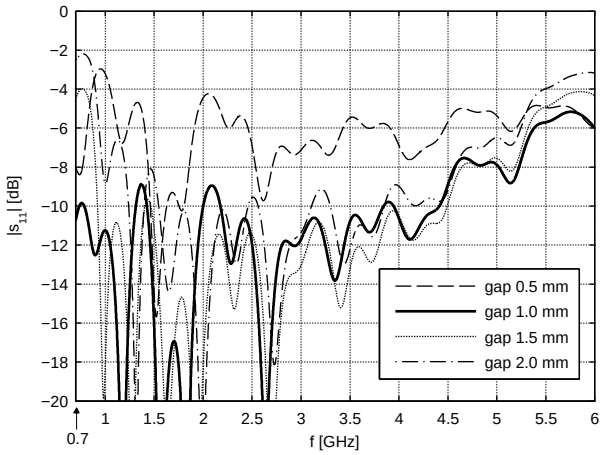

Fig. 4. Simulations for various gaps between the ridges.

influence on matching, while the radiation pattern has been found to be largely insensitive to small changes in the antenna geometry. Fine tuning of the parameters has been done using measurements on a prototype.

The flare is designed with open boundary, but includes a shorting strip similar to [7] resulting from matching optimization; the strip is 20 mm wide at a distance of 80 mm from the transition waveguide. The antenna is 348 mm long, with an aperture size of 288 mm. The ridges are tapered approximating an exponential transition between the characteristic impedance of the feeding waveguide and free space. Note that the tapering of the ridges runs right from the feed in full length of the antenna. Towards the feed the ridges are chamfered to accommodate the very narrow gap resulting from tapering and to achieve higher bandwidth and lower impedance [5].

The antenna is fed by a coaxial probe—a coaxial cable passes throughout the ridge with outer conductor connected to it and the inner conductor is attached to the opposite ridge (see Fig. 3). The passage is filled with dielectric material and keeps the characteristic impedance at 50 Ohms. There are two probes arranged perpendicularly to each other for excitation of both polarizations. The probes are positioned 2 mm apart, counting for 14 degrees of phase shift at the upper end of the frequency range.

The gap between the ridges at the feedpoint is one of the most crucial dimensions of the antenna. While the tapering length was kept constant, we eventually chose 1 mm as the optimum distance between the ridges at the feedpoint with respect to the reflection coefficient (s_{11}). We also found, however, that the tendency of the reflection coefficient is generally not monotonic with the gap width (see Fig. 4 with FDTD simulations). This is in contrast to [16] and [17] which report that the matching improves with decreasing the gap between the ridges. Exact physical explanation remains unclear to us, but we hypothesize that the size of the feed may be the cause, since the diameter of the inner conductor of the coaxial probe is 1 mm, comparable to the gap itself.

Thickness of the ridges has been determined by numerical optimization as 8 mm. Reducing the overall thickness of the ridges negatively influences the performance of the antenna and also poses some practical difficulties, e.g. does not allow

for the coaxial feeding through the ridges. However, large portion of the ridges has been milled out resulting in 2 mm thickness everywhere except a 10 mm wide frame at the edges—we did not find any significant influence of this modification. The benefit is reduced weight of the antenna, which is especially important when it is used as an array element. Another component of the antenna of which dimensions were numerically investigated was the cavity behind the feed, but again without noticing any considerable impact.

B. The Array

The antenna array presented in this paper has 16 previously described horn antennas arranged in a quasi-spherical pattern (Fig. 5), with emphasis on the coverage of the upper hemisphere. The elements in the array (schematic in Fig. 6) are arranged into 4 groups (rows) with antennas sharing the same theta angle from the vertical axis in each group. The first group contains one element pointing directly upwards, the second group has 4 elements with $\theta = 40°$, the third group has 7 elements with $\theta = 75°$, pointing slightly above the horizon, and the fourth group has 4 elements with $\theta = 110°$, pointing slightly below the horizon.

The described constellation has been chosen seeking the highest possible homogeneity in obtaining the directional channel information, but also with respect to practical matters like mounting and mobility. In particular, the lower hemisphere is not covered entirely due to the presence of the mounting rod and also because of generally lower probability of signal incoming from the downward direction. Generally, we were searching for the highest possible distance between any two antenna elements in order to minimize the coupling. The pattern homogeneity was, however, also expected to be improved by this approach. All the mounting pods for the antennas were arranged in such a way that the antennas are positioned on a sphere, i.e. with approximately equal distance from the geometrical center of the array. The homogeneity of the final array turned out to be satisfactory, as shown below in results.

III. Results

Fig. 7 shows the s_{11} parameter of the horn antenna across the intended operation frequency range, obtained by measurement and FDTD simulations. This plot is a result of extensive optimization on the shape of the antenna, as we tried to find dimensions giving maximum possible bandwidth, favorable matching and well-defined radiation beam, all at the same time. The result is s_{11} lower than -10 dB in most of the frequency range of interest and lower than -6 dB in few segments. However, there are notable differences between the measurement and the simulation which are caused by subtle mechanical changes on the final prototype (ridge gap, waveguide walls perforation) which could not be reflected in the simulation. Differences appeared also when comparing radiation patterns, therefore we decided to rely entirely on measurement in obtaining the remaining antenna parameters.

One of the most important parameters of any antenna array is the amount of mutual coupling between the array elements. The results for the worst coupling in the array (approx. $40°$

Fig. 5. The quad-ridged horn antennas in the spherical array arrangement.

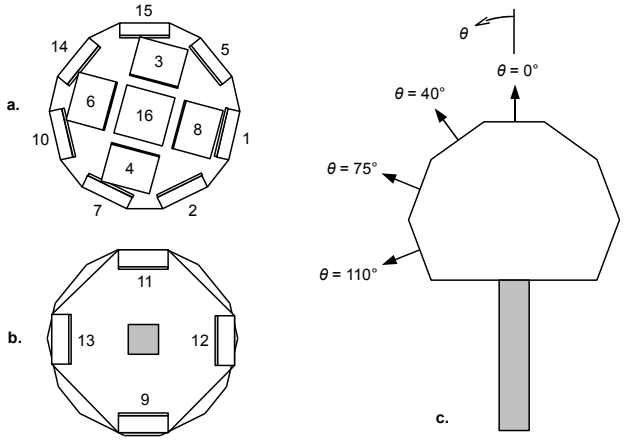

Fig. 6. Distribution and numbering of the horn antennas on the spherical array; a. top view, b. bottom view, c. theta angles of the element rows.

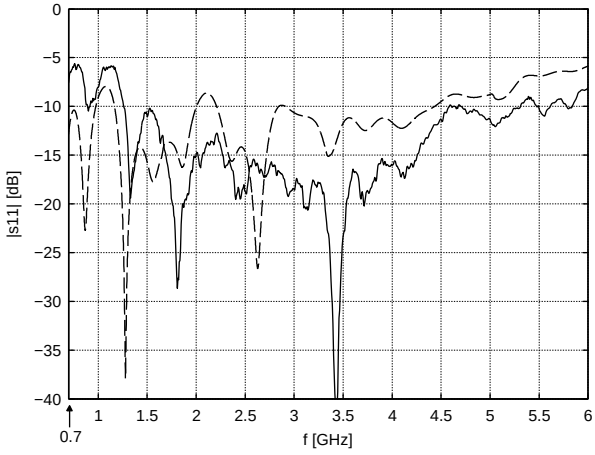

Fig. 7. Reflection coefficient (s_{11}) of the quad-ridged horn antenna. Solid line: measurement, dashed line: simulation.

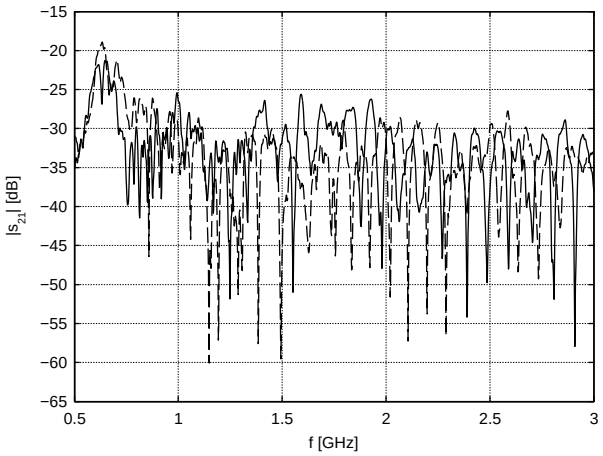

Fig. 8. Measured mutual coupling (s_{21} parameter) between the two nearest neighboring antennas (11–15) with both polarizations (solid: horizontal, dashed: vertical).

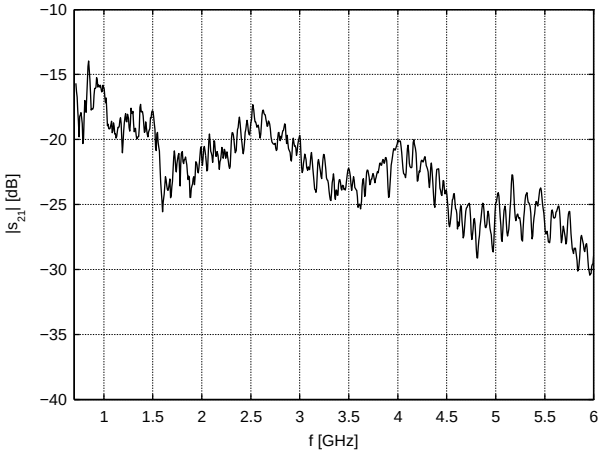

Fig. 9. Measured mutual coupling (s_{21} parameter) between the two ports of the same antenna.

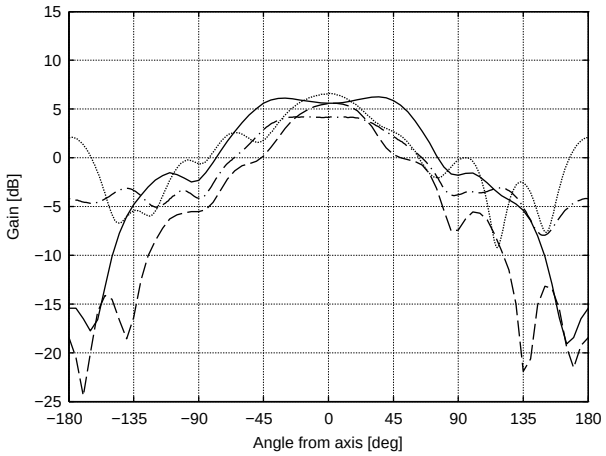

Fig. 10. Measured radiation pattern for the antenna cluster in H- (solid line) and E-plane (dashed line), and for single antenna in H- (dash-dotted line) and E-plane (dotted line), at 776 MHz.

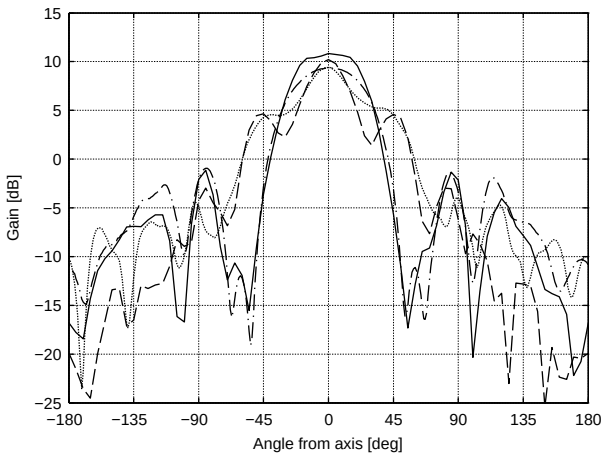

Fig. 11. Measured radiation pattern for the antenna cluster in H- (solid line) and E-plane (dashed line), and for single antenna in H- (dash-dotted line) and E-plane (dotted line), at 2.3 GHz.

apart) are shown in Fig. 8. The maximum coupling in the frequency band of interest occurs at the lower end with magnitude at most -19 dB. Only the ports with the same orientation (H-H, V-V) are significantly coupled as shown in Fig. 8, whereas mixed polarization coupling is less than -80 dB in all cases (not shown). It is the H-plane coupling (V-V) which turned out to be the strongest. The coupling between the two ports of the same antenna is shown in Fig. 9.

The radiation pattern is quite insensitive to small changes in the geometry of the antenna. However, its properties change throughout the band as it is demonstrated for four selected frequencies: 776 MHz, 2.3 GHz, 4.5 GHz and 6 GHz (see Figs. 10–13). In this case, the measurement setup consisted of the measured element and four neighboring identical antennas tilted by 40° from the main axis ("antenna cluster"), in order to capture an image of the real-world performance of the antenna as a part of the array. Radiation patterns for the single antenna only are also included in Figs. 10–13 for comparison.

The directivity (directive gain) grows with frequency (Fig. 14) and the single beam becomes narrower (Fig. 15), while the front-to-back ratio improves. The beam is generally wider in the H-plane than in the E-plane. At the upper frequency limit (6 GHz, Fig. 13) the beam is still intact with a wide flat top in H-plane and mild sidelobes in E-plane. Still, some of the sidelobes occur throughout the entire band, but these have generally lower level and they are also pointing around 40 degrees or more from the main beam, suggesting that they are caused by the influence of the four neighboring antennas.

Figs. 16–21 show the sum beams in θ- and ϕ-polarization of the whole spherical array composed of 16 horn antennas. The sum beam is obtained by summing power contributions from all of the antennas in the array and both polarization feeds. It shows how homogeneous the array will be in retrieving the directional channel information over the sphere. Each antenna is represented by a full 3D radiation pattern in both polarizations, including the influence of its four neighbors.

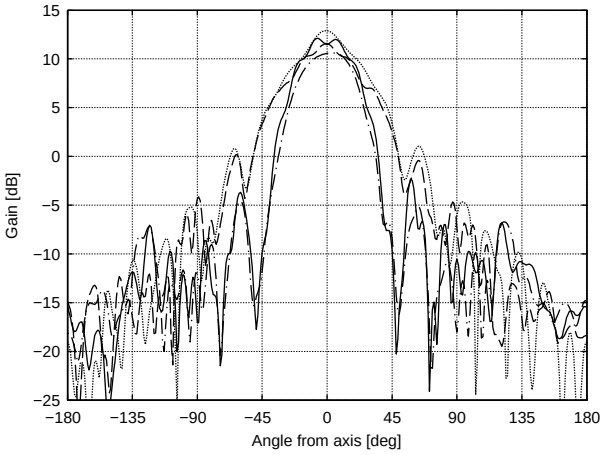

Fig. 12. Measured radiation pattern for the antenna cluster in H- (solid line) and E-plane (dashed line), and for single antenna in H- (dash-dotted line) and E-plane (dotted line), at 4.5 GHz.

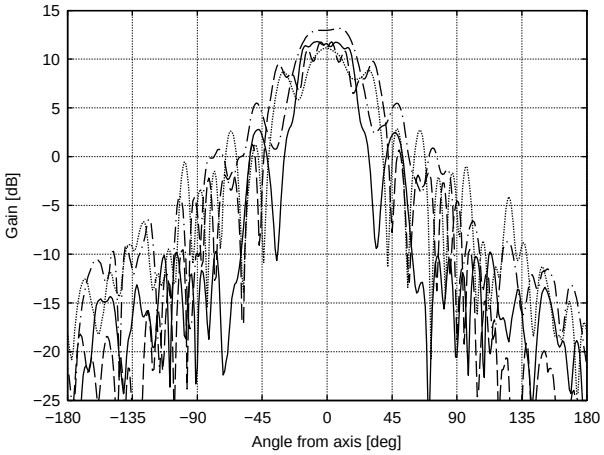

Fig. 13. Measured radiation pattern for the antenna cluster in H- (solid line) and E-plane (dashed line), and for single antenna in H- (dash-dotted line) and E-plane (dotted line), at 6 GHz.

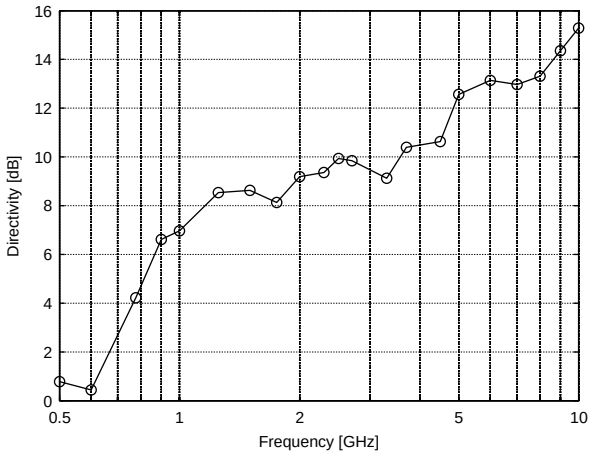

Fig. 14. Measured directivity versus frequency.

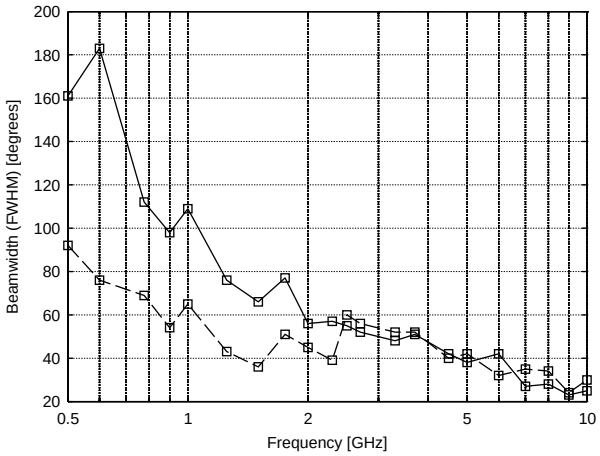

Fig. 15. Measured beamwidth (full-width half-maximum) in H- (solid line) and E-plane (dashed line) versus frequency.

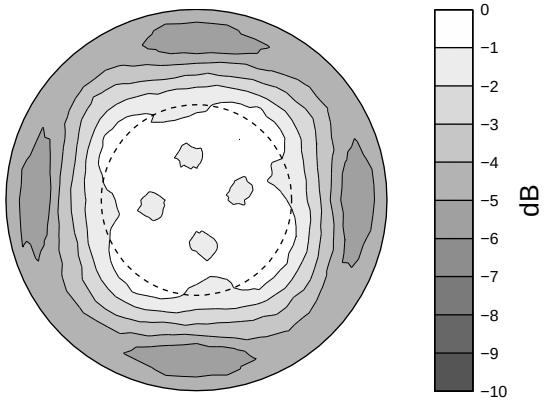

Fig. 16. Sum beam of array (relative power to maximum), θ-polarization, 776 MHz.

These patterns are then rotated into the appropriate direction and added together. The plot center in Figs. 16–21 corresponds to the "north pole" of the spherical domain (radiation upwards) while the circumference corresponds to the downwards radiation, or "south pole". The horizontal radiation, or "the equator", is denoted by a dashed line at half distance from the center to the circumference.

From the schematic of the array (Fig. 6) it follows that the coverage in the downwards direction will be minimal, and this is indeed the case. The homogeneity is generally better when the antenna beam is wider, as at the lower frequency (776 MHz, Figs. 16, 17), or when it has many secondary sidelobes, which can be observed at the upper end of the band (6 GHz, Figs. 20, 21). However, at higher frequencies there is also a higher probability of sharp dips in the sum radiation pattern. In particular, the homogeneity of the sum beam at 776 MHz is within 3 dB for upper hemisphere (inner part of the circle), while at 2.3 GHz we have only 4 dB and for 6 GHz even 6 dB span due to sporadic dips. These numbers apply to a 16-element array. For 32 and 62 elements in the array (uniform

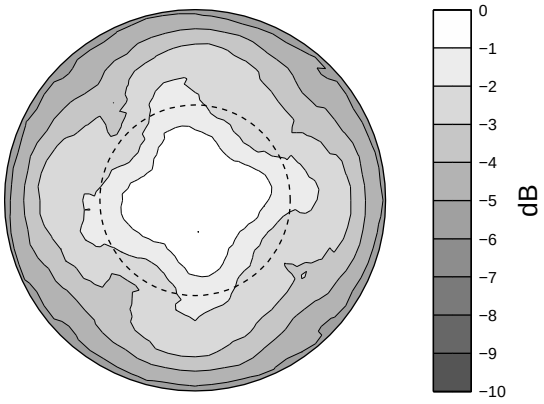

Fig. 17. Sum beam of array (relative power to maximum), ϕ-polarization, 776 MHz.

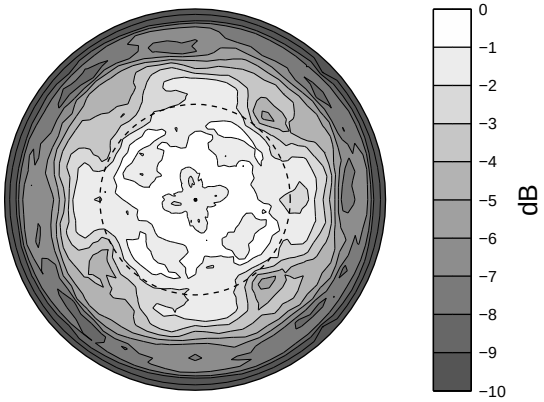

Fig. 18. Sum beam of array (relative power to maximum), θ-polarization, 2.3 GHz.

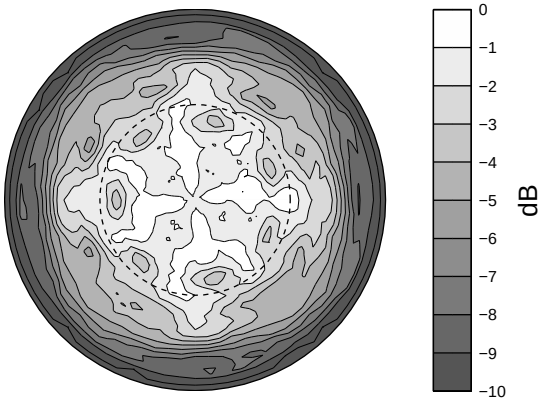

Fig. 19. Sum beam of array (relative power to maximum), ϕ-polarization, 2.3 GHz.

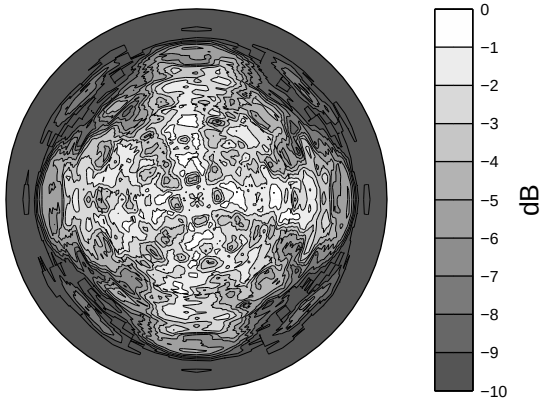

Fig. 20. Sum beam of array (relative power to maximum), θ-polarization, 6.0 GHz.

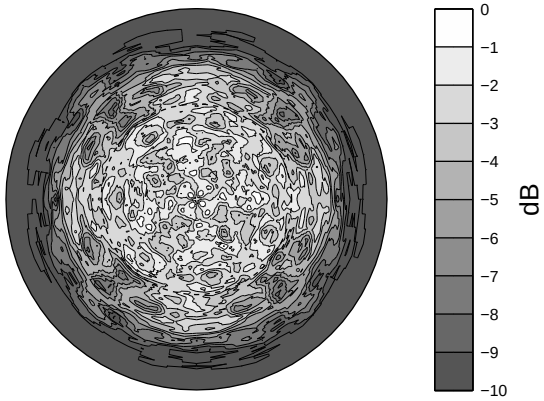

Fig. 21. Sum beam of array (relative power to maximum), ϕ-polarization, 6.0 GHz.

distribution around the sphere, not displayed) the homogeneity would be better than 6 dB and 4 dB, respectively, for both hemispheres at 6 GHz, but then the array would have a larger diameter and corresponding weight.

IV. Conclusion

In this paper, a spherical array with dual-polarized quad-ridged horn antenna as an element has been introduced. The 16-element array has an isotropy of max. 6 dB over the sum radiation pattern in the upper hemisphere within frequency range from 600 MHz to 6 GHz. The reflection coefficient of the horn antenna is below -6 dB across the frequency range and the coupling between the elements is typically better than -20 dB. The radiation pattern of a single antenna in the array shows a single well-defined beam with small sidelobes and good front-to-back ratio. The directivity reaches 12 dB for the most part of the band. Although there was a quite significant proximity effect of the neighboring antennas on the radiation pattern, this did not manifest in the coupling. We therefore conclude that the presented array is suitable

for wireless propagation studies with potential for accurate estimation of signal direction.

ACKNOWLEDGMENT

The authors would like to thank the TAP reviewers and Dr. Elisabeth de Carvalho for their useful comments on the manuscript.

REFERENCES

[1] M. Knudsen and G. Pedersen, "Spherical outdoor to indoor power spectrum model at the mobile terminal," *Selected Areas in Communications, IEEE Journal on*, vol. 20, no. 6, pp. 1156–1169, Aug 2002.

[2] K. Kalliola, H. Laitinen, L. Vaskelainen, and P. Vainikainen, "Real-time 3-d spatial-temporal dual-polarized measurement of wideband radio channel at mobile station," *Instrumentation and Measurement, IEEE Transactions on*, vol. 49, no. 2, pp. 439–448, Apr 2000.

[3] O. Franek, G. Pedersen, and J. Andersen, "Numerical modeling of a spherical array of monopoles using fdtd method," *Antennas and Propagation, IEEE Transactions on*, vol. 54, no. 7, pp. 1952–1963, July 2006.

[4] C. Balanis, *Modern antenna handbook*. Wiley-Interscience New York, NY, USA, 2008.

[5] W. Sun and C. Balanis, "Analysis and design of quadruple-ridged waveguides," *Microwave Theory and Techniques, IEEE Transactions on*, vol. 42, no. 12, pp. 2201–2207, Dec 1994.

[6] J. Kerr, "Short axial length broad-band horns," *Antennas and Propagation, IEEE Transactions on*, vol. 21, no. 5, pp. 710–714, Sep 1973.

[7] C. Bruns, P. Leuchtmann, and R. Vahldieck, "Analysis and simulation of a 1–18 GHz broadband double-ridged horn antenna," *Electromagnetic Compatibility, IEEE Transactions on*, vol. 45, no. 1, pp. 55–60, Feb 2003.

[8] V. Rodriguez, "New broadband EMC double-ridge guide horn antenna," *RF Design*, vol. 27, no. 5, 2004.

[9] M. Botello-Perez, H. Jardon-Aguilar, and I. Ruiz, "Design and simulation of a 1 to 14 GHz broadband electromagnetic compatibility drgh antenna," in *Electrical and Electronics Engineering, 2005 2nd International Conference on*, Sept. 2005, pp. 118–121.

[10] S. Soroka, "A physically compact quad ridge horn design," in *Antennas and Propagation Society International Symposium, 1986*, vol. 24, Jun 1986, pp. 903–906.

[11] Z. Shen and C. Feng, "A new dual-polarized broadband horn antenna," *Antennas and Wireless Propagation Letters, IEEE*, vol. 4, pp. 270–273, 2005.

[12] V. Rodriguez, "An open-boundary quad-ridged guide horn antenna for use as a source in antenna pattern measurement anechoic chambers," *Antennas and Propagation Magazine, IEEE*, vol. 48, no. 2, pp. 157–160, April 2006.

[13] R. Dehdasht-Heydari, H. Hassani, and A. Mallahzadeh, "Quad ridged horn antenna for UWB applications," *Progress In Electromagnetics Research*, vol. 79, pp. 23–38, 2008.

[14] ——, "A new 2-18 GHz quad-ridged horn antenna," *Progress In Electromagnetics Research*, vol. 81, pp. 183–195, 2008.

[15] A. Taflove, *Computational Electrodynamics: The Finite-Difference Time-Domain Method*, 3rd ed. Boston: Artech House, 2005.

[16] M. Abbas-Azimi, F. Arazm, and J. Rashed-Mohassel, "Sensitivity analysis of a 1 to 18 GHz broadband drgh antenna," in *Antennas and Propagation Society International Symposium 2006, IEEE*, July 2006, pp. 3129–3132.

[17] M. Kujalowicz, W. Zieniutycz, and M. Mazur, "Double-ridged horn antenna with sinusoidal ridge profile," in *Microwaves, Radar & Wireless Communications, 2006. MIKON 2006. International Conference on*, May 2006, pp. 759–762.

Ondřej Franek (S'02–M'05) was born in 1977. He received the M.Sc. (Ing., with honors) and Ph.D. degrees in electronics and communication from Brno University of Technology, Czech Republic, in 2001 and 2006, respectively. Currently, he is working at the Department of Electronic Systems, Aalborg University, Denmark, as a postdoctoral research associate. His research interests include computational electromagnetics with focus on fast and efficient numerical methods, especially the finite-difference time-domain method. He is also involved in research on biological effects of non-ionizing electromagnetic radiation, indoor radiowave propagation, and electromagnetic compatibility.

Dr. Franek was the recipient of the Seventh Annual SIEMENS Award for outstanding scientific publication.

Gert Frølund Pedersen was born in 1965, is married to Henriette and has 7 children. He received the B.Sc.E.E. degree, with honour, in electrical engineering from College of Technology in Dublin, Ireland, and the M.Sc.E.E. and Ph.D. degrees from Aalborg University in 1993 and 2003. He has been employed by Aalborg University since 1993 where he is now full Professor heading the Antennas, Propagation and Radio Networking group and is also the head of the doctoral school on wireless which has close to 100 Ph.D. students enrolled. His research has focused on radio communication for mobile terminals, and especially on small antennas, diversity systems, propagation and biological effects, and he has published more than 75 peer reviewed papers and holds 20 patents. He has also worked as consultant for developments of more than 100 antennas for mobile terminals including the first internal antenna for mobile phones in 1994 with lowest SAR, first internal triple-band antenna in 1998 with low SAR and high TRP and TIS, and lately various multi antenna systems rated as the most efficient on the market.

He has been one of the pioneers in establishing the over-the-air measurement systems. The measurement technique is now well established for mobile terminals with single antennas and he is now chairing the COST2100 SWG2.2 group with liaison to 3GPP for over-the-air tests of MIMO terminals.